HHS Public Access

Author manuscript

J Neurooncol. Author manuscript; available in PMC 2019 September 26.

Published in final edited form as:

J Neurooncol. 2014 January ; 116(2): 373–379. doi:10.1007/s11060-013-1304-2.

Altered functional connectivity of the default mode network in diffuse gliomas measured with pseudo-resting state fMRI

Robert J. Harris,
UCLA Brain Tumor Imaging Laboratory, Department of Radiological Sciences, David Geffen School of Medicine, University of California, Los Angeles, 924 Westwood Blvd, Suite 615, Los Angeles, CA 90024, USA

Department of Biomedical Physics, University of California, Los Angeles, Los Angeles, CA, USA

Susan Y. Bookheimer,
Department of Psychology, University of California, Los Angeles, Los Angeles, CA, USA

Timothy F. Cloughesy,
Department of Neurology, University of California, Los Angeles, Los Angeles, CA, USA

Hyun J. Kim,
UCLA Brain Tumor Imaging Laboratory, Department of Radiological Sciences, David Geffen School of Medicine, University of California, Los Angeles, 924 Westwood Blvd, Suite 615, Los Angeles, CA 90024, USA

Whitney B. Pope,
UCLA Brain Tumor Imaging Laboratory, Department of Radiological Sciences, David Geffen School of Medicine, University of California, Los Angeles, 924 Westwood Blvd, Suite 615, Los Angeles, CA 90024, USA

Albert Lai,
Department of Neurology, University of California, Los Angeles, Los Angeles, CA, USA

Phioanh L. Nghiemphu,
Department of Neurology, University of California, Los Angeles, Los Angeles, CA, USA

Linda M. Liau,
Department of Neurosurgery, David Geffen School of Medicine, University of California, Los Angeles, Los Angeles, CA, USA

Benjamin M. Ellingson
UCLA Brain Tumor Imaging Laboratory, Department of Radiological Sciences, David Geffen School of Medicine, University of California, Los Angeles, 924 Westwood Blvd, Suite 615, Los Angeles, CA 90024, USA

Department of Biomedical Physics, University of California, Los Angeles, Los Angeles, CA, USA

Department of Bioengineering, Henry Samueli School of Engineering and Applied Science, University of California, Los Angeles, Los Angeles, CA, USA

bellingson@mednet.ucla.edu.

Abstract

The purpose of the current study was to explore whether brain tumors disrupt the integrity of the default mode network (DMN), a well-characterized resting-state fMRI network. We evaluated whether tumor grade, volume, post-surgical/clinical status, or location decreased the functional connectivity within the DMN in patients with gliomas. Task-based fMRI data was obtained from 68 diffuse glioma patients and 12 healthy volunteers. Pseudo-resting state fMRI data was calculated from task-based fMRI data using standard techniques. Data was preprocessed and DMN integrity was compared across WHO grade, tumor volume surgical status (new vs. recurrent tumors), age, and KPS using univariate and multivariate linear models. WHO grade was the most significant predictor of DMN integrity ($P = 0.004$), whereas T2 hyperintense lesion volume was not a predictor ($P = 0.154$). DMN integrity was lower in high-grade (WHO III–IV) compared with low-grade (WHO II) patients ($P = 0.020$). Tumors in the left parietal lobe showed a more impaired DMN compared with tumors in the frontal lobe, while tumors within and outside the network nodes did not differ significantly. Results suggest higher tumor grade along with prior surgery and/or treatment cause the largest reduction in DMN functional connectivity in patients with primary gliomas, and that tumor location has an impact on connectivity.

Keywords

Functional connectivity; Resting-state fMRI; Brain tumors; Glioma

Introduction

Approximately 22,500 cases of primary brain tumors are diagnosed each year; of these, approximately 70 % are malignant gliomas [1]. Malignant gliomas often exhibit a high degree of tumor cell infiltration and proliferation compared with lower grade gliomas [2]. Tumor cells produce or recruit matrix metalloproteinases that mediate extracellular matrix degradation [3], allowing tumor cells to migrate through the parenchyma and infiltrate into regions of the brain. This microscopic infiltration, otherwise undetectable by traditional imaging sequences, is thought to be the primary reason for dismal prognosis in malignant gliomas. As such, more advanced MR techniques such as DTI and fMRI have been investigated for applicability in noninvasive assessment of tumor burden.

Resting state fMRI has emerged as a reproducible and unbiased way of measuring the functional connectivity between different regions of the brain. Even in the absence of stimulus (i.e. the resting state), studies have identified multiple correlated networks in the brain associated with various functions [4]. The most easily detected and consistent of these is the default mode network (DMN), a network consisting of four primary nodes approximately located in the anterior cingulate cortex (ACC), posterior cingulated cortex (PCC), left lateral parietal cortex (LLPC), and right lateral parietal cortex (RLPC) [5–8]. The reproducibility of this network across patients and studies makes it a target of interest in functional connectivity research. Although the precise implications of alterations in this network are not fully understood, numerous studies have shown alterations in the DMN in neurological conditions including Alzheimer's Disease [9], schizophrenia [10], and dementia [11]. As neurological and personality changes are known to accompany tumor

growth and infiltration and functional connectivity mapping using resting state fMRI has been shown to be one of the most powerful methods for evaluating neurological integrity of many cognitive networks [12], we hypothesized that gliomas may cause significant alterations in DMN connectivity, and that gliomas of differing aggressiveness and location may alter connectivity to different degrees.

"Pseudo" resting state fMRI is a widely accepted post-processing technique involving subsequent analysis of the *residual* fMRI signals after activation due to the task has been taken into consideration [13]. Fair et al. [13], Fox et al. [14] and Arfanakis et al. [15]. have all demonstrated that much of the variance observed in task-based fMRI experiments can be accounted for by the underlying resting state fMRI spontaneous activity. In other words, task-based fMRI is thought to consist of a linear combination of task-related activation and persistent resting spontaneous activity. In the current study we propose examining connectivity of the DMN using pseudo-resting state fMRI analysis applied to pre-operative, task-based fMRI data.

In the current study we tested the hypothesis that patients with primary brain tumors will have a lower overall functional connectivity between nodes of the DMN compared with healthy patients, and that connectivity between nodes distal from the tumor mass will also be altered. We hypothesize that high grade gliomas will result in greater deterioration of the DMN network, potentially related to their more invasive nature. Additionally, we hypothesize that tumor volume and post-surgical status (newly diagnosed vs. recurrent) may also influence DMN integrity.

Methods

Patients

A total of 68 patients with histologically confirmed gliomas and 12 healthy control volunteers were examined in this study. Of the 68 patients, 21 had World Health Organization (WHO) grade II gliomas, 14 were WHO grade III, and 33 were WHO grade IV (glioblastoma) (Table 1). Patient data was retrospectively obtained from our institutional database and had been acquired between 2007 and 2012 for pre-surgical planning purposes. Patients were filtered to include only those with left hemisphere and/or frontal lobe gliomas. A small number of patients with right hemispheric tumors were excluded from further analysis in order to provide a more homogeneous patient population. Of the low-grade glioma patients (average age, 36; average Karnofsky Performance Score (KPS), 91), 12 out of 21 patients were newly diagnosed (57 %) and 9 of 21 patients had fMRI at tumor recurrence (43 %). A total of 23 of 47 (49 %) high-grade glioma patients (average age, 53; average KPS, 86) were newly diagnosed and 24 of 47 (51 %) patients had fMRI at recurrence. All patients were on minimal steroids prior to surgery.

MRI acquisition and pre-processing

All patients underwent anatomical T2WI and T1WI MPRAGE scans as well as multiple task-based fMRI scans (TR = 2,500, TE = 35, flip angle = 90°, 128 × 128 matrix size) of a uniform timing paradigm: alternating 10-s blocks of rest and stimulus, with a total scan time

of 4 min (96 acquisitions). The stimulus task was one of the following, based on available retrospective data: (i) a right- or left-handed finger tapping task; (ii) a right- or left-footed foot tapping task; (iii) a visual or audio response task; (iv) an object naming task; (v) a tongue-moving task. All functional data underwent preprocessing consisting of the following steps: (i) truncation of the first five time points to allow for magnetization equilibrium; (ii) application of a 0.01 Hz high-pass filter; (iii) motion correction of the series to the first time point using MCFLIRT (FSL [16]; FMRIB, Oxford, UK); (iv) interleaved slice timing correction; and v) spatial smoothing of 5 mm full-width half-maximum. For each time series, the stimulus paradigm was then deconvolved from the raw data using the *3dDeconvolve* function in AFNI (Analysis of Functional Neuro-Images, afni.nimh.nih.gov) [17]. The resulting "pseudoresting state fMRI data" [13] and anatomical T2-weighted images were then registered to the T1-weighted Montreal Neurological Institute (MNI) atlas. The three pseudo-resting state fMRI time series datasets were then concatenated and used for connectivity analysis. Data from healthy volunteers was acquired using a single fMRI paradigm (an alternating 10-s finger tapping task) with similar acquisition parameters, deconvolution, preprocessing and registration processes as tumor patient data.

Image processing

Tumor volume was defined by hyperintensity on T2-weighted images using a semiautomated thresholding technique followed by manual adjustment of the contour in AFNI. ROIs for the four primary nodes of the DMN were defined via a DMN template provided by the GIFT toolbox for Matlab [18], which was registered to standard MNI template space. A 10 mm spherical ROI was placed at the center of each of those locations in MNI template space. For both patients and healthy controls, the mean pseudo-resting state fMRI time series data within each ROI was calculated for each DMN node. The mean pseudo-resting state fMRI time series for each node was correlated with signals from the other nodes using a Pearson's correlation coefficient (r), resulting in a total of six connectivity measurements between the four nodes (Fig. 1). These correlation coefficients were then converted to z-scores using a Fisher transformation [19, 20]. The six z-score values were averaged to obtain a global DMN connectivity measurement for each participant.

Statistics

Univariate linear analysis was used to separately test the influence of tumor volume, surgical status (newly diagnosed vs. recurrent), WHO grade, age, and KPS on global DMN connectivity. A multivariate analysis was also performed to compare all five variables and identify the strongest predictors of DMN integrity. Tumor volumes were compared between high (WHO III–IV) and low grade (WHO II). Global DMN connectivity of WHO grade II, III, and IV tumor patients, along with healthy volunteers, were computed and compared using a one-way ANOVA and Tukey's test for multiple comparisons. High-grade patients were then separated into three groups based on tumor location; these were organized as patients with a tumor in the LLPC node ($n = 19$), patients with a tumor in the ACC node ($n = 8$), and patients with a left hemisphere tumor outside the DMN ($n = 20$). Global DMN connectivity and T2 hyperintense lesion volume were compared between these groups using a one-way ANOVA. Patients with a tumor in either node ($n = 27$) were then combined and

compared against patients with a tumor outside the DMN ($n = 20$). For low-grade tumors, we examined the difference between tumors within ($n = 8$) and outside ($n = 13$) the DMN as well, although the within-DMN group was not split into three tumor location groups for ANOVA due to lack of sufficient group size. Lastly, for both the high-grade and low-grade tumor groups, newly diagnosed glioma patients were compared with recurrent patients to test for a significant difference in global DMN connectivity.

Results

Univariate analysis suggested that WHO grade ($P = 0.004$) significantly influenced global DMN connectivity and surgical status (newly diagnosed vs. recurrent, $P = 0.064$) was trending towards significance, whereas T2 hyperintense lesion volume was not ($P = 0.154$). Age ($P = 0.637$) and KPS ($P = 0.248$) also did not significantly influence global DMN connectivity. Multivariate analysis supported these trends, illustrating that WHO grade was the most significant predictor of DMN integrity ($P = 0.012$), although surgical status was no longer trending (newly diagnosed vs. recurrent; $P = 0.248$). T2 hyperintense lesion volume ($P = 0.995$), age ($P = 0.103$), and KPS ($P = 0.293$) were still not significant factors in multivariate analysis. As expected, T2 lesion volume was higher in malignant gliomas compared with low grade gliomas (t test, $P < 0.001$). One-way ANOVA revealed a significant difference between global DMN connectivity in grade II, III and IV patients and healthy controls (Fig. 2a; $P < 0.0001$). In particular, results identified a trend of decreasing global DMN connectivity with increasing WHO grade (Healthy, mean = 0.78; grade II, 0.58; grade III, 0.54; grade IV, 0.45). Tukey's test for multiple comparisons suggested differences between the healthy group and all three tumor groups (vs. WHO II, $P < 0.01$; vs. WHO III, $P < 0.01$; vs. WHO IV, $P < 0.001$). In general, a decrease in DMN connectivity was observed in high-grade compared with low-grade gliomas (Fig. 2b; t test, $P = 0.020$).

High-grade gliomas demonstrated a significant difference in global DMN connectivity based on tumor location (Fig. 3; ANOVA, $P = 0.006$). Specifically, patients with tumors in the LLPC had a significantly lower overall DMN connectivity compared to patients with tumors in the ACC (Tukey's test, $P < 0.01$). Volumes were significantly different between tumors outside the DMN and within either the LLPC or ACC node (t test, $P < 0.0001$), but tumors located within the LLPC and ACC nodes did not significantly differ in volume (t test, $P = 0.914$). Mean global DMN connectivity for tumors located within the LLPC, within the ACC, and outside all DMN nodes were 0.40, 0.60, and 0.49, respectively. A difference in global DMN connectivity between tumors within or outside DMN nodes was not observed for either the high-grade (t test, $P = 0.495$) or low-grade gliomas (t test, $P = 0.923$).

Lastly, we tested whether global DMN connectivity was altered as a result of previous surgical and/or chemotherapeutic intervention, specifically comparing newly diagnosed versus recurrent gliomas. As expected, global DMN connectivity was significantly lower in recurrent glioma patients (Fig. 4a; t test, $P = 0.015$). When stratified by malignancy, the trend of lower DMN connectivity in recurrent tumors was trending towards significance in high-grade gliomas (Fig. 4b; t test, $P = 0.051$) but not low-grade gliomas (Fig. 4b; t test, $P = 0.839$). The observation of statistical differences in DMN connectivity in newly diagnosed versus recurrent high-grade gliomas may be due to addition of radiochemotherapy in high

grade gliomas prior to recurrence; whereas low-grade gliomas are not treated as aggressively with radiation or chemotherapy.

Discussion

Although a few studies have examined the applicability of resting state fMRI for presurgical planning of the sensorimotor and networks [19, 21, 22], to the best of our knowledge, this is the first study to investigate DMN integrity in brain tumor patients using resting state fMRI, and the first to explore the correlation between functional connectivity and tumor grade. Our findings suggest that DMN integrity is impaired as a result of tumor, and that WHO grade and surgical status are significantly correlated with DMN integrity. Interestingly, our results suggest that tumor volume plays only a minimal role in alteration of the DMN network, and DMN integrity may be also influenced by tumor location.

Results from the current study support the hypothesis that degree of tumor malignancy (WHO grade) is highly correlated with the integrity of the DMN. Malignant gliomas are associated with infiltration into surrounding brain parenchyma, resulting in damage to regions of the brain that may be involved in neurological function. Although this invasion is often ill defined on standard MR imaging techniques, resting state fMRI measures of functional connectivity may provide additional insight into the degree of tumor infiltration. Interestingly, our results failed to find a strong statistical association between DMN connectivity and tumor size on T2-weighted images. Although speculative, these results suggest that large T2 lesions may not necessarily disrupt the DMN if they do not have histopathological features of malignancy, but rather may displace neural connections between functional regions. Alternatively, tumors appearing small on T2-weighted images and presenting with aggressive histopathological features may damage neural connections between functional regions. T2-enhancing lesions comprise both edematous tissue and tumor, and the relative contribution of each to a particular patient's lesion volume is unknown when contouring. As edema and tumor may disrupt neural networks in differing ways, this may explain our lack of correlation as well.

Interestingly, high-grade gliomas located within the ACC demonstrated a stronger global connectivity compared with gliomas located within the LLPC or outside the DMN nodes altogether, despite no difference in tumor volume between the high-grade LLPC and ACC groups. This finding may reflect the larger physical distance of the ACC node from other DMN nodes, reducing the influence of infiltrating tumor on the other nodes.

Post-surgical status (i.e. newly diagnosed vs. recurrent gliomas) also significantly influenced DMN integrity. Specifically, patients who were evaluated after a first surgical resection and upon recurrence (prior to second surgery) demonstrated a lower global DMN connectivity compared with newly diagnosed glioma patients. This result may reflect the influence of physical tissue damage and removal; however, this result may also reflect the fact that recurrent gliomas tend to be treatement-resistive, hypoxia-tolerant, and more aggressive than pre-treatment gliomas. Additionally, due to the retrospective nature of this study, post-surgical patients in some cases received a variety of radiotherapy or chemotherapy following surgery, which may have altered cognition and white matter integrity.

There were several important limitations to this study. First, only task-based fMRI data was available for analysis, from which the pseudo-resting state fMRI signal was generated. While task-based data is beneficial for a retrospective study due to its more common acquisition in brain tumor patients than true resting-state data, previous studies have shown that task-induced correlations may contaminate the resting correlations in pseudo-resting state fMRI data and that constant engagement of a task may alter underlying spontaneous BOLD fluctuations, resulting in underestimation of the strength of connectivity in resting-state networks [23]. Regardless, the differences in connectivity observed under various conditions in the current study appear to be large enough even with this potential contamination from task-based activity. An additional limitation in the current study was lack of age matched healthy control participants to our patient population and the low-grade glioma group was of a lower mean age than the high-grade group. In general, studies have shown a decrease in DMN activity that accompanies normal aging [24–27], although the magnitude of change in the DMN observed due to normal aging is substantially less than we observed in our patient population. Another important limitation in the current study was lack of post-contrast T1-weighted images at the same time point as fMRI data. The lack of a significant trend between DMN integrity and tumor volume may be a result of this limitation, as tumor burden is typically defined by contrast-enhancement on post-contrast T1-weighted images. We did not correct our images for mass effect, which may have resulted in physical misalignment of brain tissue compromising the DMN nodes in some patients with larger tumors. Lastly, in future studies, it would be beneficial to perform neuro-cognitive testing near the date of MRI acquisition to supplement our current findings, as well as diffusion tensor imaging in order to determine whether the distance of the tumor to specific white matter tracts influences connectivity.

Conclusions

There remains a clinical need for noninvasive assessment of cognitive function in glioma patients. Resting-state fMRI is a novel, unbiased method of assessing global cognitive integrity. Results from the current study suggest that tumor grade, location, and post-surgical status significantly altered functional connectivity in the default mode network, whereas T2 hyperintense lesion volume did not appear to play a significant role in DMN connectivity.

Funding

NIH/NCI R21CA167354 (BME); UCLA Institute for Molecular Medicine Seed Grant (BME); UCLA Radiology Exploratory Research Grant (BME); University of California Cancer Research Coordinating Committee Grant (BME); ACRIN Young Investigator Initiative Grant (BME); Art of the Brain (TFC); Ziering Family Foundation in memory of Sigi Ziering (TFC); Singleton Family Foundation (TFC); and Clarance Klein Fund for Neuro-Oncology (TFC).

References

1. Wen PY, Kesari S (2008) Malignant gliomas in adults. N Engl J Med 359:492–507 [PubMed: 18669428]
2. Claes A, Idema AJ, Wesseling P (2007) Diffuse glioma growth: a guerilla war. Acta Neuropathol 114:443–458 [PubMed: 17805551]
3. Ennis BW, Matrisian LM (1994) Matrix degrading metalloproteinases. J Neurooncol 18:105–109 [PubMed: 7964973]

4. Damoiseaux JS, Rombouts SA, Barkhof F, Scheltens P, Stam CJ, Smith SM, Beckmann CF (2006) Consistent resting-state networks across healthy subjects. Proc Natl Acad Sci USA 103:13848–13853 [PubMed: 16945915]
5. Greicius MD, Krasnow B, Reiss AL, Menon V (2003) Functional connectivity in the resting brain: a network analysis of the default mode hypothesis. Proc Natl Acad Sci USA 100:253–258 [PubMed: 12506194]
6. Bellec P, Perlbarg V, Jbabdi S, Pelegrini-Issac M, Anton JL, Doyon J, Benali H (2006) Identification of large-scale networks in the brain using fMRI. Neuroimage 29:1231–1243 [PubMed: 16246590]
7. Chen S, Ross TJ, Zhan W, Myers CS, Chuang KS, Heishman SJ, Stein EA, Yang Y (2008) Group independent component analysis reveals consistent resting-state networks across multiple sessions. Brain Res 1239:141–151 [PubMed: 18789314]
8. Otti A, Gundel H, Wohlschlager A, Zimmer C, Sorg C, Noll-Hussong M (2012) Default mode network of the brain. Neurobiology and clinical significance. Nervenarzt 83(16):18–24
9. Zhu DC, Majumdar S, Korolev IO, Berger KL, Bozoki AC (2013) Alzheimer's disease and amnestic mild cognitive impairment weaken connections within the default-mode network: a multi-modal imaging study. J Alzheimers Dis 34:969–984 [PubMed: 23313926]
10. Waltz JA, Kasanova Z, Ross TJ, Salmeron BJ, McMahon RP, Gold JM, Stein EA (2013) The roles of reward, default, and executive control networks in set-shifting impairments in schizophrenia. PLoS ONE 8:e57257 [PubMed: 23468948]
11. Filippi M, Agosta F, Scola E, Canu E, Magnani G, Marcone A, Valsasina P, Caso F, Copetti M, Comi G, Cappa SF, Falini A (2012) Functional network connectivity in the behavioral variant of frontotemporal dementia. Cortex 49(9):2389–2401 [PubMed: 23164495]
12. Rogers BP, Morgan VL, Newton AT, Gore JC (2007) Assessing functional connectivity in the human brain by fMRI. Magn Reson Imaging 25:1347–1357 [PubMed: 17499467]
13. Fair DA, Schlaggar BL, Cohen AL, Miezin FM, Dosenbach NU, Wenger KK, Fox MD, Snyder AZ, Raichle ME, Petersen SE (2007) A method for using blocked and event-related fMRI data to study "resting state" functional connectivity. Neuroimage 35:396–405 [PubMed: 17239622]
14. Fox MD, Snyder AZ, Zacks JM, Raichle ME (2006) Coherent spontaneous activity accounts for trial-to-trial variability in human evoked brain responses. Nat Neurosci 9:23–25 [PubMed: 16341210]
15. Arfanakis K, Cordes D, Haughton VM, Moritz CH, Quigley MA, Meyerand ME (2000) Combining independent component analysis and correlation analysis to probe interregional connectivity in fMRI task activation datasets. Magn Reson Imaging 18:921–930 [PubMed: 11121694]
16. Smith SM, Jenkinson M, Woolrich MW, Beckmann CF, Behrens TE, Johansen-Berg H, Bannister PR, De Luca M, Drobnjak I, Flitney DE, Niazy RK, Saunders J, Vickers J, Zhang Y, De Stefano N, Brady JM, Matthews PM (2004) Advances in functional and structural MR image analysis and implementation as FSL. Neuroimage 23(Suppl 1):S208–S219 [PubMed: 15501092]
17. Cox RW (1996) AFNI: software for analysis and visualization of functional magnetic resonance neuroimages. Comput Biomed Res 29:162–173 [PubMed: 8812068]
18. Franco AR, Pritchard A, Calhoun VD, Mayer AR (2009) Inter-rater and intermethod reliability of default mode network selection. Hum Brain Mapp 30:2293–2303 [PubMed: 19206103]
19. Otten ML, Mikell CB, Youngerman BE, Liston C, Sisti MB, Bruce JN, Small SA, McKhann GM 2nd (2012) Motor deficits correlate with resting state motor network connectivity in patients with brain tumours. Brain 135:1017–1026 [PubMed: 22408270]
20. Fisher RA (1921) On the "probable error" of a coefficient of correlation deduced from a small sample. Metron 1:3–32
21. Shimony JS, Zhang D, Johnston JM, Fox MD, Roy A, Leuthardt EC (2009) Resting-state spontaneous fluctuations in brain activity: a new paradigm for presurgical planning using fMRI. Acad Radiol 16:578–583 [PubMed: 19345899]
22. Zhang D, Johnston JM, Fox MD, Leuthardt EC, Grubb RL, Chicoine MR, Smyth MD, Snyder AZ, Raichle ME, Shimony JS (2009) Preoperative sensorimotor mapping in brain tumor patients using spontaneous fluctuations in neuronal activity imaged with functional magnetic resonance imaging: initial experience. Neurosurgery 65:226–236 [PubMed: 19934999]

23. Fransson P (2006) How default is the default mode of brain function? Further evidence from intrinsic BOLD signal fluctuations. Neuropsychologia 44:2836–2845 [PubMed: 16879844]

24. Wu JT, Wu HZ, Yan CG, Chen WX, Zhang HY, He Y, Yang HS (2011) Aging-related changes in the default mode network and its anti-correlated networks: a resting-state fMRI study. Neurosci Lett 504:62–67 [PubMed: 21925236]

25. Andrews-Hanna JR, Snyder AZ, Vincent JL, Lustig C, Head D, Raichle ME, Buckner RL (2007) Disruption of large-scale brain systems in advanced aging. Neuron 56:924–935 [PubMed: 18054866]

26. Damoiseaux JS, Beckmann CF, Arigita EJ, Barkhof F, Scheltens P, Stam CJ, Smith SM, Rombouts SA (2008) Reduced resting-state brain activity in the “default network” in normal aging. Cereb Cortex 18:1856–1864 [PubMed: 18063564]

27. Persson J, Lustig C, Nelson JK, Reuter-Lorenz PA (2007) Age differences in deactivation: a link to cognitive control? J Cogn Neurosci 19:1021–1032 [PubMed: 17536972]

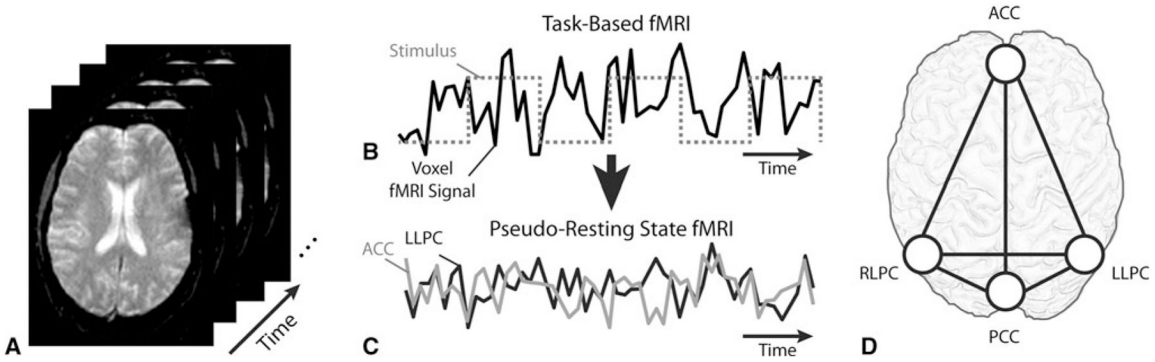

Fig. 1.

a Task-based fMRI data consists of rapid echoplanar (EPI) acquisition over time during a stimulus. **b** To isolate the pseudo-resting state fMRI signal, the fMRI stimulus block design (*gray dashed line*) is first convolved with a hemodynamic response function and then deconvolved with the fMRI time-series data in each image voxel (*black*). **c** The residual signal after deconvolution is used to as pseudo-resting state fMRI data. From this pseudo-resting state fMRI data, voxels in each region of interest identified as part of the default mode network nodes are averaged to get a single fMRI time-series for each node. The functional connectivity between the average pseudo-resting state fMRI time series in each node is then calculated using a Pearson's correlation coefficient, *r*. **d** Recognized nodes within the DMN include the ACC, PCC, LLPC, and RLPC

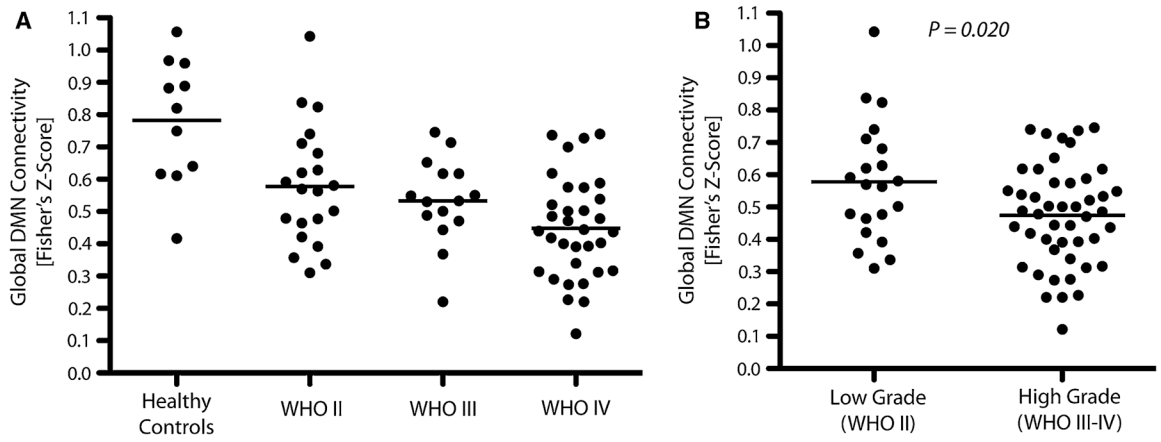

Fig. 2.

a Global DMN connectivity for healthy volunteers and tumor patients by grade (One-way ANOVA, $P < 0.0001$). **b** Global DMN connectivity in low grade (WHO II) and high-grade (WHO III-IV) gliomas (*t* test, $P = 0.020$)

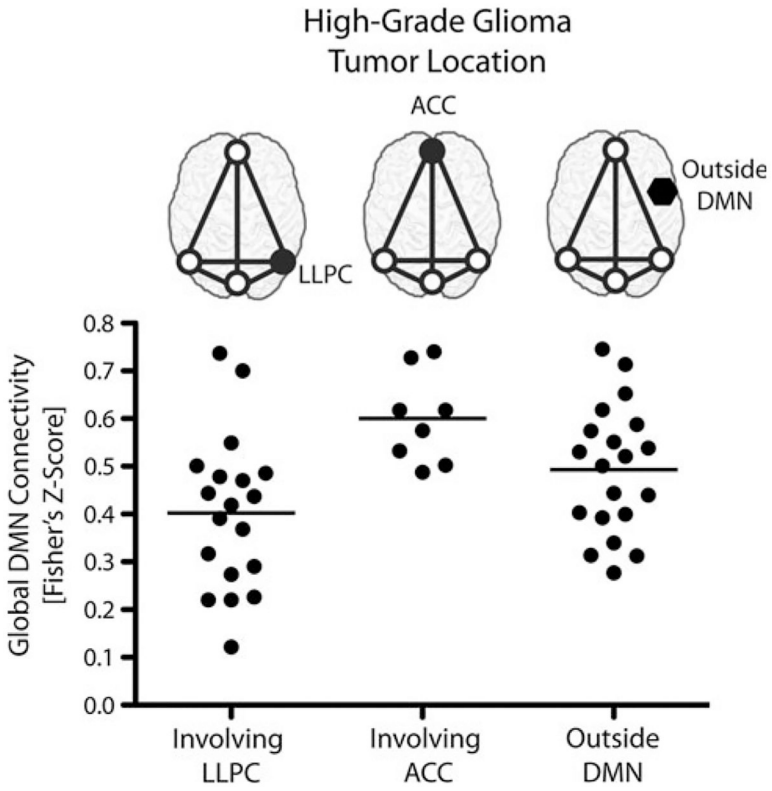

Fig. 3.

Global DMN connectivity by tumor location in high-grade gliomas (One-way ANOVA, $P = 0.006$)

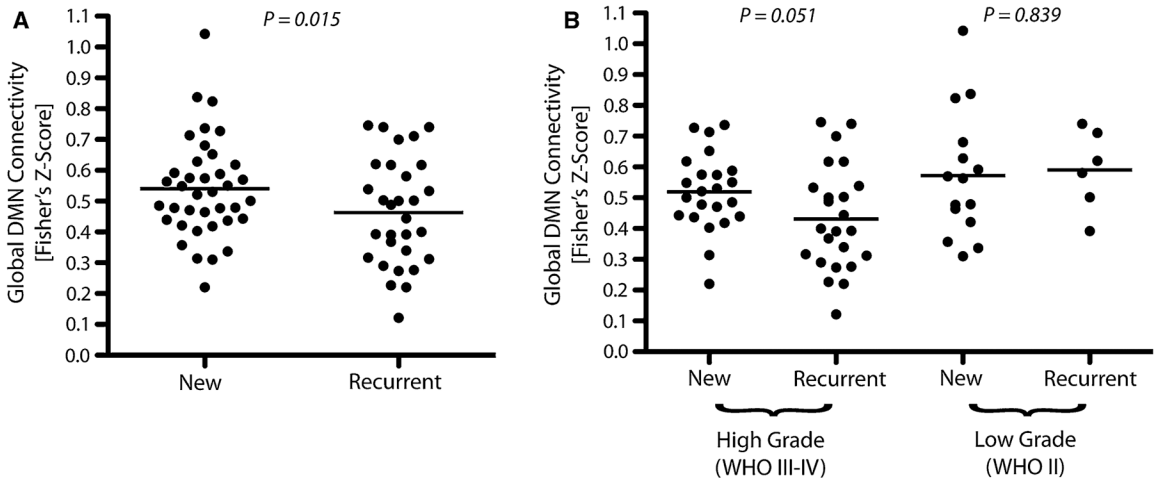

Fig. 4.

a Global DMN connectivity in newly diagnosed and recurrent glioma patients for all tumor grades (*t* test, $P = 0.015$). **b** Global DMN connectivity for newly diagnosed and recurrent glioma patients stratified by high- (WHO III–IV; *t* test, $P = 0.051$) or low-grade (WHO II; *t* test, $P = 0.839$)

Table 1

Glioma patient cohort by grade and tumor location

Total patients	Tumor grade	Tumor location
n = 68	WHO II, *n* = 21	LLPC, *n* = 3
		ACC, *n* = 5
		Outside DMN, *n* = 13
	WHO III, *n* = 14	LLPC, *n* = 3
		ACC, *n* = 4
		Outside DMN, *n* = 7
	WHO IV, *n* = 33	LLPC, *n* = 16
		ACC, *n* = 4
		Outside DMN, *n* = 13